

# miR-888 is an expressed prostatic secretions-derived microRNA that promotes prostate cell growth and migration

Holly Lewis<sup>1</sup>, Raymond Lance<sup>1,2</sup>, Dean Troyer<sup>1</sup>, Hind Beydoun<sup>3</sup>, Melissa Hadley<sup>1</sup>, Joseph Orians<sup>1</sup>, Tiffany Benzine<sup>1</sup>, Kenya Madric<sup>1</sup>, O John Semmes<sup>1</sup>, Richard Drake<sup>1,†</sup>, and Aurora Esquela-Kerscher<sup>1,\*</sup>

<sup>1</sup>Department of Microbiology & Molecular Cell Biology; Leroy T. Canoles Jr. Cancer Research Center; Eastern Virginia Medical School; Norfolk, VA USA; <sup>2</sup>Department of Urology; Eastern Virginia Medical School and Urology of Virginia; Norfolk, VA USA; <sup>3</sup>Graduate Program in Public Health; Eastern Virginia Medical School; Norfolk, VA USA

<sup>†</sup>Current affiliation: Department of Cell and Molecular Pharmacology and Experimental Therapeutics; Medical University of South Carolina; Charleston, SC USA

**Keywords:** non-coding RNA, microRNA, miRNA, miR-888, prostate, prostate cancer, expressed prostatic secretions urine, EPS urine

microRNAs (miRNAs) are a growing class of small non-coding RNAs that exhibit widespread dysregulation in prostate cancer. We profiled miRNA expression in syngeneic human prostate cancer cell lines that differed in their metastatic potential in order to determine their role in aggressive prostate cancer. miR-888 was the most differentially expressed miRNA observed in human metastatic PC3-ML cells relative to non-invasive PC3-N cells, and its levels were higher in primary prostate tumors from cancer patients, particularly those with seminal vesicle invasion. We also examined a novel miRNA-based biomarker source called expressed prostatic secretions in urine (EPS urine) for miR-888 expression and found that its levels were preferentially elevated in prostate cancer patients with high-grade disease. These expression studies indicated a correlation for miR-888 in disease progression. We next tested how miR-888 regulated cancer-related pathways in vitro using human prostate cancer cell lines. Overexpression of miR-888 increased proliferation and migration, and conversely inhibition of miR-888 activity blocked these processes. miR-888 also increased colony formation in PC3-N and LNCaP cells, supporting an oncogenic role for this miRNA in the prostate. Our data indicates that miR-888 functions to promote prostate cancer progression and can suppress protein levels of the tumor suppressor genes RBL1 and SMAD4. This miRNA holds promise as a diagnostic tool using an innovative prostatic fluid source as well as a therapeutic target for aggressive prostate cancer.

## Introduction

Prostate cancer remains the most prevalent form of non-skin cancer in males within the United States and is the second leading cause of cancer deaths in men despite the widespread use of prostate specific antigen (PSA) as a diagnostic test for prostate cancer.<sup>1</sup> Population-based PSA screening can result in the overdiagnosis and overtreatment of prostate cancer as well as failure to identify men with aggressive forms of the disease.<sup>1-3</sup> Indeed, after ~18 y of routine PSA screening, the United States Preventive Services Task Force has recommended that routine PSA testing in men be discontinued.<sup>4</sup> More accurate biomarkers are required that can discriminate between indolent and lethal forms of prostate cancer and allow men with the highest risk to seek aggressive treatment earlier during the course of their disease. MicroRNAs (miRNAs) have recently emerged as promising diagnostic biomarkers and therapeutic targets for prostate cancer.<sup>5</sup> These ~22 nucleotide non-coding RNAs do not encode for proteins and yet play essential roles in controlling growth

and differentiation in human cells. There are over 2500 mature miRNAs identified in the human genome to date (miRBase, ver. 20<sup>6</sup>), and many of these small RNAs are misexpressed in a wide range of human cancers and contribute to tumor formation and metastasis.<sup>7,8</sup> miRNAs generally act to negatively regulate gene expression by binding to complementary sequences within their target messenger RNAs (mRNAs), resulting in a block in protein translation and/or mRNA degradation of the target.<sup>9,10</sup> Growing functional evidence supports a role for miRNAs as tumor suppressor genes and oncogenes in various organ systems.<sup>7,8</sup>

Little is known regarding how miRNAs contribute to cancer progression and metastasis, specifically in the prostate. Studies analyzing the deregulation of miRNA expression in prostate tumors and immortalized prostate cancer cell lines indicate unique “miRNA signatures” that can differentiate between diseased and non-cancer patients and potentially serve as biomarkers for prostate cancer.<sup>5,11,12</sup> miRNAs have also been detected in body fluids, including serum, plasma, urine, and saliva, and are

\*Correspondence to: Aurora Esquela-Kerscher; Email: kerschae@evms.edu  
Submitted: 10/23/2013; Accepted: 10/28/2013  
<http://dx.doi.org/10.4161/cc.26984>

being explored as diagnostics in these non-invasive sources for this disease.<sup>13-18</sup> Profiling studies using microarrays, quantitative real-time PCR (qRT-PCR), and next-generation deep sequencing have identified prostate cancer-associated miRNAs that potentially contribute to the underlying etiology of the disease, e.g., the tumor suppressor miRNAs; *let-7*, miR-200 family, miR-15a/miR-16-1, miR-101, miR-449, and miR-99 family and the oncogenic miRNAs; miR-21, miR-221/222, and miR-32.<sup>13,19-29</sup> There is less known about miRNAs' influence on prostate cancer metastasis—a clinical condition currently incurable and lethal for patients. miRNAs such as miR-200, miR-203, miR-205, miR-34a, and miR-29b are reported to suppress prostate metastasis. However, there remains a poor understanding of how miRNAs promote advanced disease and metastatic processes in this tissue.<sup>29-34</sup>

In the present study, we identified miRNAs that correlated with aggressive forms of prostate cancer by profiling global miRNA expression using TaqMan-based microfluidic arrays for 2 syngeneic human prostate cancer PC3 sublines, the metastatic PC3-ML and non-invasive PC3-N cells.<sup>35</sup> These miRNA expression studies led us to characterize miR-888, a novel prostate cancer-associated miRNA that was enriched in aggressive PC3-ML cells and elevated in primary prostate tumors from prostate cancer patients. We tested miRNA expression in a newly developed fluid biomarker source called expressed prostatic secretions in post-DRE urine (EPS urine), and noted that miR-888 levels were differentially elevated in EPS urine from prostate cancer patients with high-grade disease. Furthermore, miR-888 played a functional role in the prostate, and we found that miR-888 induced proliferation, migration, and colony formation of human prostate cancer cells. Our results also showed that miR-888 repressed protein levels of the tumor suppressor genes RBL1 and SMAD4. This work indicates that miR-888 functions to promote prostate cancer progression and is a novel clinical target for aggressive disease.

**Table 1.** MicroRNAs differentially expressed in PC3 sublines using TaqMan low-density arrays

PC3-ML vs. PC3-N		PC3-N vs. PC3-ML	
miRNA	Fold change	miRNA	Fold change
hsa-miR-888	841.5	hsa-miR-375	61.8
hsa-miR-495	433.6	hsa-miR-551b	17.2
hsa-miR-485-3p	316.6	hsa-miR-330-5p	14.7
hsa-miR-891a	283.8	hsa-miR-190	14.3
hsa-miR-517c	113.6	hsa-miR-142-3p	8.2
hsa-miR-505	78.7	hsa-miR-22	5.7
hsa-miR-34a	64.5	hsa-miR-627	5.5
hsa-miR-509-5p	16.7	hsa-miR-519a	5.4
hsa-miR-296-5p	14.4	hsa-miR-582-5p	4.6
hsa-miR-503	12.0	hsa-miR-570	3.7
hsa-miR-486-5p	9.4	hsa-miR-215	3.6
hsa-miR-423-5p	6.7	hsa-miR-219-1-3p	3.5

Note: miRNAs showed enriched expression for both experimental trials and possessed a standard deviation lower than the fold-change. \*For a complete listing of results see **Tables S1 and 2**.

## Results

### Identification of miRNAs associated with aggressive prostate cancer

A screen to identify miRNAs that correlated with aggressive prostate cancer was performed by comparing expression profiles in 2 syngeneic human prostate cancer cell lines that differed in their metastatic potential. We focused on PC3-ML, an aggressive, hormone-refractory PC3-derived cell line that consistently metastasizes to the lumbar vertebrae when injected into immunocompromised mice, as well as PC3-N, a non-invasive PC-3 derived cell line with low metastatic potential (gift from Dr M Stearns).<sup>35</sup> The expression of 377 human miRNAs in PC3-ML and PC3-N cells were measured using microfluidic miRNA TaqMan qRT-PCR Low-Density Arrays (Human Array A Card; Applied Biosystems). Forty-seven miRNAs exhibited significantly higher ( $\geq 3$ -fold) expression in the PC3-ML cells vs. the PC3-N cells, the most notable being miR-888 (hsa-miR-888-5p) (**Table 1**, top 12 miRNAs shown based on 2 independent trials for each cell line; **Tables S1 and S2** list complete data sets.) Conversely, 12 miRNAs showed significant enrichment in the non-invasive PC3-N cells relative to metastatic PC3-ML cells (**Table 1**). We hypothesized that the differentially expressed miRNAs represented unique signatures that distinguished for aggressive characteristics of human prostate cancer cells. A subset of prostate cancer-associated miRNAs upregulated in the metastatic PC3-ML cells, e.g., miR-148a,<sup>36</sup> miR-27a,<sup>37</sup> miR-221,<sup>38</sup> miR-34a,<sup>32</sup> and miR-330,<sup>39</sup> were previously found to be associated with aggressive prostate disease and/or androgen responsiveness. Additional uncharacterized miRNAs identified in our profiling study, such as miR-888, could also play a functional role in the progression of prostate cancer cells to metastatic, lethal disease.

### miR-888 showed elevated expression in human prostate cancer cell lines and primary prostate tumors from cancer patients

Individual qRT-PCR assays were used to re-verify the megaplex

TaqMan microfluidic array results for select miRNAs and test the reliability of this high-throughput screening platform. We confirmed that miR-888 was significantly higher in metastatic PC3-ML cells relative to the non-invasive PC3-N subline (**Fig. 1B**), implicating a novel role for miR-888 in prostate cancer progression. miR-888 is a conserved member of the miR-743 family with no characterized function. This miRNA resides within a genomic cluster consisting of 7 miRNAs on human chromosome Xq27.3 that were initially classified as epididymis-specific genes<sup>40-42</sup> (**Fig. 1A**). We noted that an additional member of the miR-888 cluster, miR-891a, was similarly expressed at higher levels in PC3-ML relative to PC3-N cells in both the TaqMan Low Density Arrays (**Table 1**)

and singleplex TaqMan qRT-PCR (Fig. 1B). We therefore focused our analysis on these 2 clustered miRNAs in the human prostate.

We went on to compare the expression of miR-888 and cluster member miR-891a in immortalized prostate cell lines that differed in their hormone sensitivity. This is clinically relevant, because prostate tumor cells, which rely on androgens for growth and survival, eventually become resistant to castration or hormonal deprivation therapies and are incurable. We investigated if miR-888 and miR-891a were preferentially elevated in hormone refractory prostate cancer cell lines compared with androgen-sensitive cell lines. miR-888 and miR-891a expression in these studies were measured relative to RWPE-1, a transformed prostate epithelial cell line that lacks the ability to form tumors.<sup>43</sup> Both miR-888 and miR-891a were present at low levels (relative to RWPE-1) in the androgen-responsive prostate cancer cell lines LNCaP and PacMetUT1<sup>44</sup> (Fig. 1C; Fig. S1A). In contrast, these miRNAs showed significantly elevated expression in the castration-resistant PC3 parental line and its derivatives, PC3-ML and PC3-N.<sup>35</sup> We also noted differential expression within the PC3 derivatives. miR-888 and miR-891a expression levels were elevated in the PC3 parental line and considerably higher in the more aggressive PC3-ML subline.

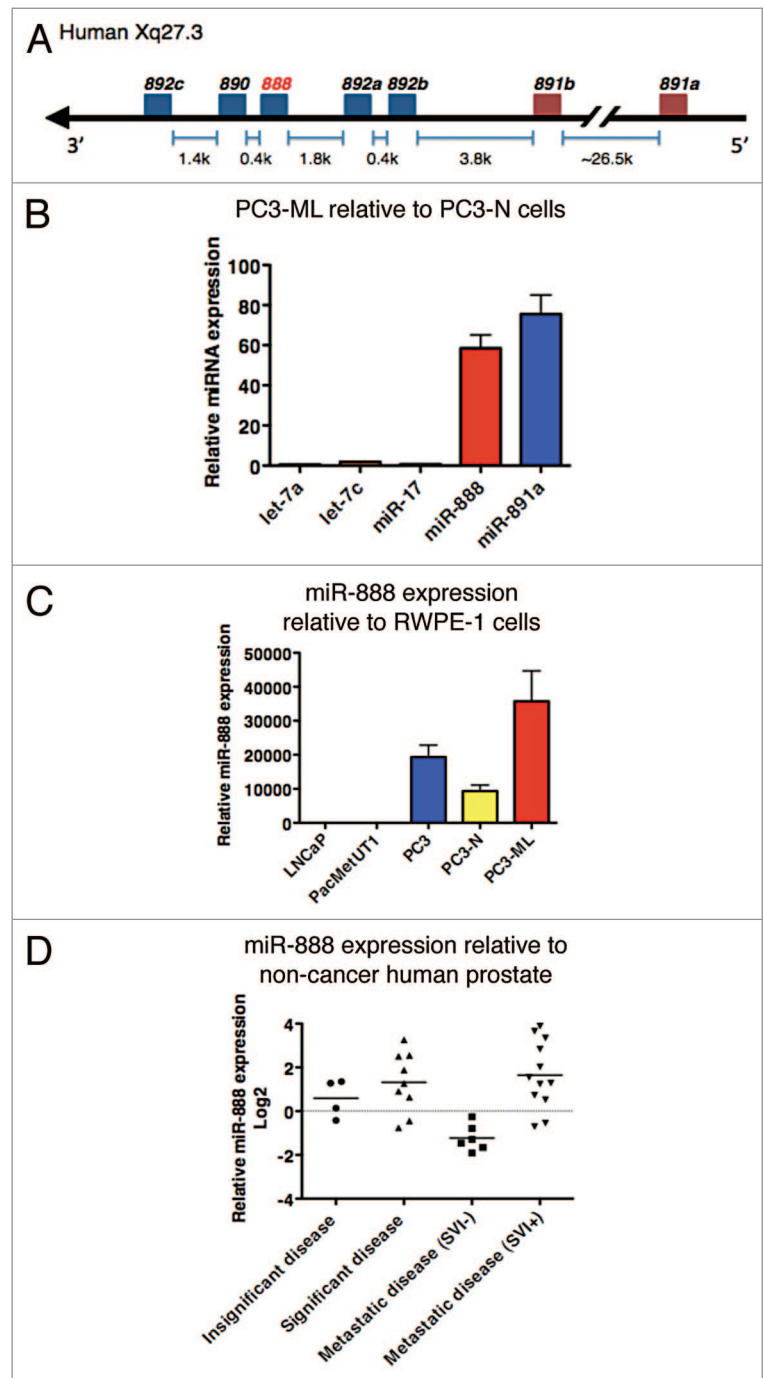
We investigated if miR-888 and miR-891a were abnormally modulated in primary prostate tissues taken from cancer patients compared with non-cancer patients. Primary prostate tumor specimens used in this analysis represented a spectrum of the disease ranging from indolent to lethal prostate cancer: insignificant disease (tumor size  $\leq 0.5$  cc, pathological stage  $\leq T2$ , Gleason  $\leq 6$ ), significant organ-confined disease (tumor size  $\geq 0.5$  cc, pathological stage T2, any Gleason, 5 y follow-up with no metastasis or biochemical recurrence), and metastatic disease (confirmed distant metastasis). miR-888 expression (but not miR-891a) tended to be higher in primary prostate tumors relative to normal prostate tissue by TaqMan-based qRT-PCR (Fig. 1D; Fig. S1B).

**Figure 1.** miR-888 is expressed in human prostate cancer cell lines and primary prostate tumors. (A) miR-888 resides within a cluster of 7 miRNAs on the minus strand of human chromosome Xq27.3 that spans a length of about 34 kilobases (k). (B) Individual TaqMan-based qRT-PCR reactions verified enrichment of miR-888 and miR-891a in aggressive PC3-ML cells vs. non-invasive PC3-N prostate cancer cell lines. (C) miR-888 expression levels were higher in hormone refractory PC3-derived prostate cancer cell lines (PC3, PC3-N, PC3-ML) compared with androgen-sensitive cell lines (LNCaP and PacMetUT1). Results were normalized to RNU48 and expression was relative to non-malignant prostate epithelial RWPE-1 cells. (D) De-identified human prostate tumor formalin-fixed, paraffin-embedded (FFPE) tissues from distinct clinical groups—insignificant disease, significant organ-confined prostate cancer, and metastatic disease (separated by patients diagnosed with [SVI+] or without [SVI-] seminal vesicle invasion following prostatectomy)—showed modulated miR-888 expression relative to non-cancerous prostate tissue by qRT-PCR. Baseline at point 0 is the average of 3 non-prostate cancer patients. In (B–D), qRT-PCR was performed in triplicate and error bars represent mean + standard deviation (SD).

Within the metastatic group, we noted that patients who presented with seminal vesicles invasion following prostatectomy showed higher relative miR-888 expression in their primary tumors than those without seminal vesicle invasion. This finding could be clinically significant, since prostate cancer associated with seminal vesicle infiltration is considered a pathological marker for poor patient outcome and higher risk of metastatic disease post-prostatectomy.<sup>45–48</sup>

#### miR-888 expression in EPS urine correlated with high-grade disease in prostate cancer patients

EPS urine is a novel miRNA-based biomarker source. It is collected non-invasively via urine capture following gentle



massage of the prostate gland during a routine digital rectal exam (DRE). Massage stimulates the release of prostatic fluids and detached epithelial cells directly into the urethra.<sup>49,50</sup> EPS urine-derived biomarkers could be used to identify patients at high risk for aggressive, lethal forms of prostate cancer in the early diagnostic period. We therefore analyzed the expression of cancer-associated miRNAs in EPS urine, particularly miR-888, which we found were modulated in human prostate cell lines differing in their metastatic potential. In this study, we separated EPS urine specimens into supernatant and pellet fractions by low speed centrifugation and measured miRNA expression using TaqMan-based qRT-PCR. miRNA expression in the supernatant fraction of EPS urine specimens had not been previously studied. We thus needed to optimize RNA isolation procedures for the EPS urine supernatants and normalized these samples by

spiking-in *C. elegans* miRNA miR-39 (sharing no homology to human miRNAs) prior to RNA isolation. We tested our profiling methods on EPS urine by measuring the expression of miRNAs known to be widely expressed and to play a functional role in cancer progression, i.e., *let-7*, miR-16, miR-17, miR-21, and miR-125b.<sup>8,51-53</sup> We detected these miRNAs within EPS urine supernatant by qRT-PCR using a minimum sample volume of 500  $\mu$ L (Fig. S3A, miR-125b shown). This volume also allowed for reliable measurement of miRNA expression (Fig. S3B). In addition, we found that these miRNAs were stable in EPS urine, and their expression levels changed little for up to 48 h in temperatures up to 37 °C (Fig. 2A, miR-17 shown; Fig. S3C).

We investigated the expression of miR-888 as well as additional prostate cancer-associated miRNAs in EPS urine pools grouped based on clinical grade: non-cancer (24 patients), cancer

(Gleason 6–7, 25 patients, Gleason 8, 1 patient), and high-grade cancer (Gleason 9–10, 6 patients) (Fig. S4). miRNAs significantly up- or down-regulated in EPS urine supernatant from patients with high-grade relative to lower-grade prostate cancer were determined using 1-way ANOVA with Tukey Multiple Comparison Test (Fig. S5). For example, we found that *let-7c* and miR-200b levels were significantly decreased in EPS urine supernatant pools from high-grade cancer compared with lower-grade cancer patients (measured relative to EPS urine supernatant from non-cancer patients) (Fig. 2B). Our results correlated with previous profiling studies using prostate tissues and cell lines, which showed that decreased expression of *let-7c* and miR-200b closely associated with more aggressive prostate cancer phenotypes.<sup>11,22,54</sup> We also analyzed our 2 novel prostate cancer-associated miRNAs, miR-888, and miR-891a, in the EPS urine supernatant fractions to determine if their expression correlated with disease status. miR-888 levels, but not miR-891a, were higher in EPS urine obtained from high-grade cancer vs. lower-grade cancer pools (Fig. 2C). We then tested miR-888, *let-7c*, and miR-200b expression in the pellet fraction of EPS urine specimens, which was normalized to the small nucleolar RNAs (snoRNAs), RNU44 and RNU48. Unlike our results profiling the EPS urine supernatants, miRNA expression levels in the EPS urine

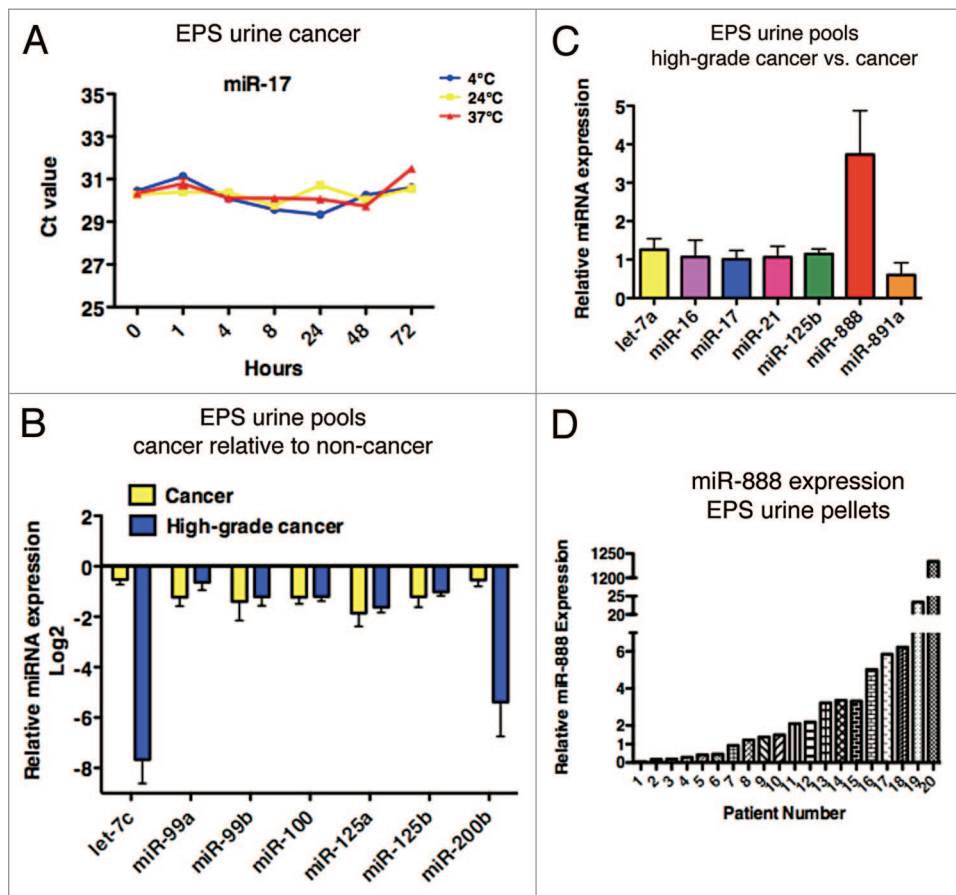


**Figure 2.** miR-888 expression in EPS urine correlated with high-grade prostate cancer. (A) miRNAs such as miR-17 were stable in EPS urine supernatant incubated at various temperatures for up to 48 h using optimized methods to analyze small RNAs by qRT-PCR in this novel fluid source. (Complete data for miR-17, miR-16, and miR-125b using EPS urine from cancer and non-cancer patients is shown in Fig. S3) (B) Cancer-associated miRNAs were analyzed in EPS urine supernatant pools from high-grade cancer (Gleason 9–10) and lower-grade cancer patients relative to non-cancer patients by qRT-PCR. *let-7c* and miR-200b were significantly reduced in EPS urine supernatant from patients with high-grade disease. (Complete data set summarized in Fig. S4) (C) miR-888, but not miR-891a, was significantly elevated in EPS urine supernatant pools from patients with high-grade relative to lower-grade prostate cancer patients. EPS urine supernatant samples in (A–C) were normalized by spiking-in 50 fM *C. elegans* miR-39. (D) 13/20 patients with prostate cancer showed increased expression of miR-888 in EPS urine pellets relative to levels found in non-cancer patients. Pellet specimens were normalized to the mean of RNU44 and RNU48 expression and delta Ct values shown.

pellets failed to correlate with clinical grade or show significant differences between cancer and non-cancer patients (Fig. 2D; Fig. S6). It was noted, however, that miR-888 levels were increased in 13/20 (65%) patients with prostate cancer relative to non-cancer patients (Fig. 2D). Taken together, EPS urine supernatant is a promising biomarker source for non-coding RNAs,

such as miR-888 (as well as *let-7c* and miR-200b), that could be used to discriminate for advanced prostate cancer.

**In vitro assays indicate an oncogenic role for miR-888 in the prostate**

Elevated miR-888 expression in human prostate cell lines, primary tumors, and EPS urine correlated with prostate cancer and

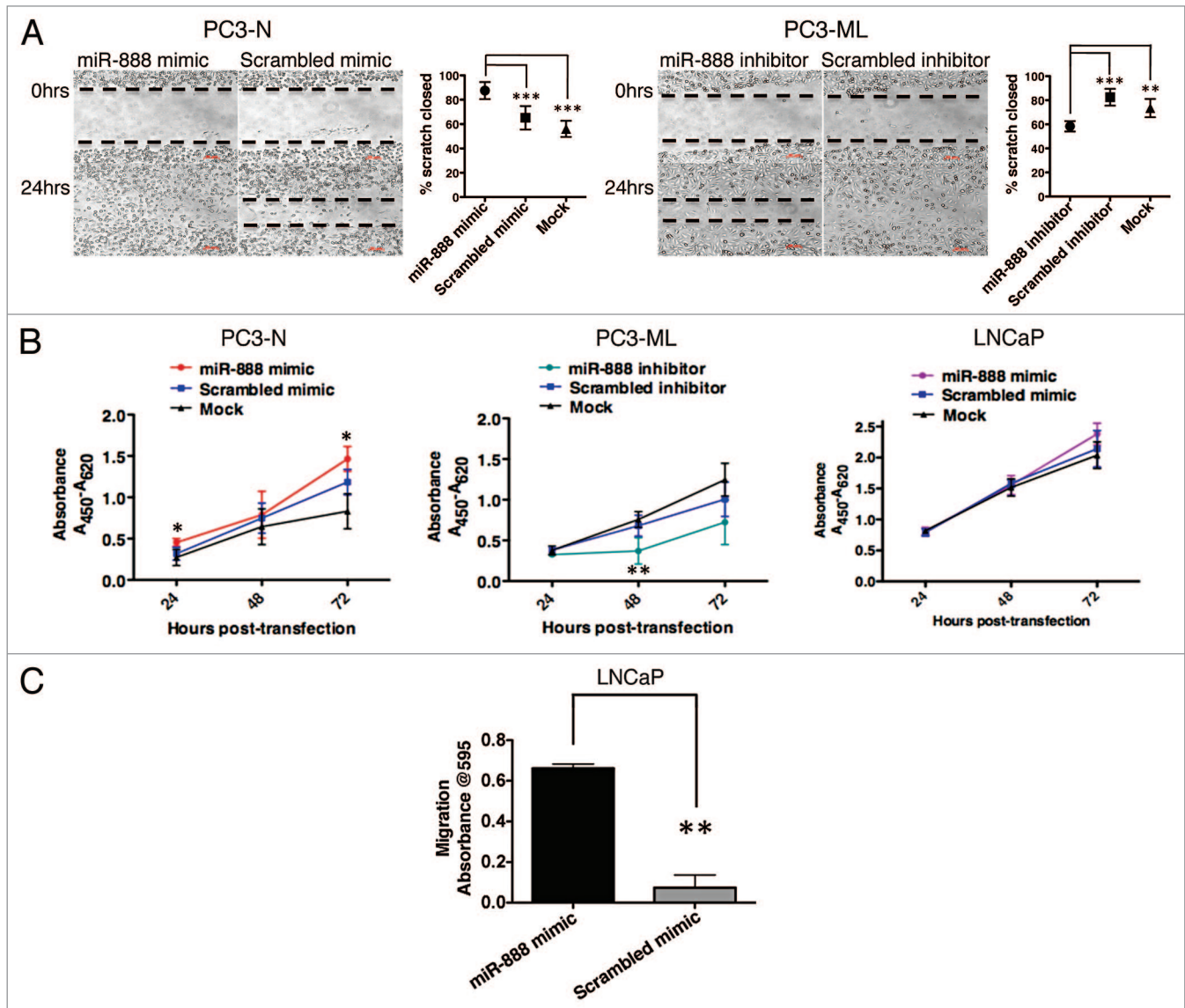


**Figure 3.** miR-888 promotes migration and proliferation of human prostate cancer cells. (A) Scratch assays show PC3-N cells (left panel) treated with miR-888 mimic migrated faster 24 h after the scratch was made than cells transfected with a scrambled mimic or mock-treated controls. Reciprocal effects were obtained when PC3-ML cells (right panel) were transfected with miR-888 inhibitor. Results are from 3 independent trials ( $n \geq 7$  for mimic, inhibitor, scrambled, and mock controls for each trial) and data depicted as column mean graphs with error bars showing confidence intervals. (B) PC3-N cells (left panel) transfected with miR-888 mimic showed increased proliferation compared with cells transfected with a scrambled mimic or mock-treated controls. Conversely, PC3-ML cells (middle panel) transfected with miR-888 inhibitor repressed proliferation rates compared with controls over a similar time-course. Moderately increased proliferation was observed in LNCaP cells (right panel) transfected with miR-888 mimic compared with scrambled or mock-treated cells. Cells were incubated with WST-1 and assayed 24, 48, and 72 h after transfection. Each graph represents 2 independent trials performed in triplicate and error bars show SD and  $P$  values shown are comparisons for miR-888 mimic/inhibitor vs. scrambled control cells (not shown:  $P$  values for miR-888 mimic vs. mock-treated at 24 and 72 h was  $P < 0.01$  and  $P < 0.001$ , respectively; and for miR-888 inhibitor vs. mock-treated at 48 and 72 h was  $P < 0.001$  and  $P < 0.0001$ , respectively.) For (A and B), \* $P$ , 0.05, \*\* $P < 0.01$ , \*\*\* $P < 0.001$ ;  $P$  values obtained by 1-way ANOVA with a Tukey post-test. (C) Boyden chamber transwell migration assays. LNCaP cells treated with miR-888 mimics possessed significantly increased migration rates 24 h post-transfection compared with cells treated with scrambled mimic controls. One of two independent trials ( $P = 0.0060$  and  $P = 0.0177$ , respectively,  $t$  test) is shown and error bars represent SD. In (A–C), transfections of mimic, inhibitor, or scrambled controls were at a concentration of 50 nM.

implicated a role for this miRNA in aggressive forms of prostate disease. We therefore investigated the function of miR-888 in the prostate and a potential connection between miR-888 misexpression and the molecular etiology of prostate cancer. Our biological studies initially focused on the castration-resistant PC3-derived cell lines that we noted expressed higher levels of miR-888 in the metastatic PC3-ML cells compared with the non-invasive PC3-N cells (Fig. 1B). We hypothesized that if miR-888 was involved in promoting cancer progression pathways in the prostate, then synthetic overexpression of this miRNA would change the behavior of PC3-N cells to a more aggressive phenotype. Conversely, repressing miR-888 activity in the metastatic PC3-ML subline would have the opposite functional effects. We overexpressed miR-888 in PC3-N cells by transfecting them with miR-888 precursor mimics (50 nM, Ambion Pre-miRNA Precursor, Life Technologies) and assayed for cell migration. Scratch (wound-healing) assays in Figure 3A (left panel) showed that PC3-N cells overexpressing miR-888 migrated faster than scrambled mimic or mock-treated control cells. Conversely, when metastatic PC3-ML cells were transfected with miR-888 inhibitors (50 nM, Dharmacon miRIDIAN MicroRNA Hairpin Inhibitor, Thermo Scientific) to block endogenous miR-888 activity, these cells migrated slower than controls over the same time period (Fig. 3A, right panel). Furthermore, miR-888 overexpression had significant migration effects in androgen-sensitive LNCaP human prostate cancer cells, as measured by Boyden chamber transwell migration assays (Fig. 3C). We also tested a role for

miR-888 in regulating prostate cell growth. Overexpression of miR-888 significantly increased proliferation rates (WST-1 assays) in PC3-N cells and moderately in LNCaP cells (Fig. 3 left and right panels). Conversely, miR-888 inhibitors transfected into PC3-ML cells repressed proliferation when compared with controls (Fig. 3, middle panel). The influence of miR-888 on cellular growth did not appear to involve the apoptosis pathway (Fig. S2). miR-888 overexpression failed to modulate the proportion of cells undergoing programmed cell death by Annexin V analysis, as shown for PC3-N cells assayed 24 h post-transfection with miR-888 mimic (50 nM) compared with controls. We subsequently tested the role of miR-888 on anchorage-independent growth of prostate cancer cells in soft agar. miR-888 significantly increased colony formation in these assays when overexpressed in both the PC3-N and LNCaP cell lines (Fig. 4). These results support the notion that miR-888 is an oncogenic factor that promotes prostate cancer progression pathways.

We were interested in identifying factors that miR-888 negatively modulates in the prostate to understand why misregulation of this miRNA was associated with prostate cancer. We identified predicted miR-888 targets possessing 3' UTR miRNA binding sites in their mRNA transcripts using the bioinformatic algorithm TargetScan. This list of potential targets was narrowed further by focusing on candidates that were also reported in the literature to be downregulated in patients with advanced forms of prostate cancer and possessed tumor-suppressive or anti-metastatic roles in the prostate, i.e., KLF5,<sup>55</sup> LMTK2,<sup>56</sup> MYCBP,<sup>57</sup> NUDT11,<sup>56</sup>

PAGE4,<sup>58,59</sup> PATE,<sup>60</sup> PMEPA1,<sup>61</sup> RBL1,<sup>62,63</sup> SMAD4,<sup>64</sup> and SRD5A.<sup>58</sup> We tested 2 of these tumor suppressor genes in the prostate for possible modulation by miR-888 in vitro; retinoblastoma like 1 (RBL1/p107), a negative cell cycle-regulatory factor possessing 1 miR-888 complementary binding site, and SMAD4, an intracellular TGF- $\beta$  signaling molecule with 2 predicted miR-888 binding sites in its 3'UTR (Fig. 5A). Briefly, PC3-N cells were harvested 24 h following treatment with miR-888 mimic (40 nM), scrambled mimic, or mock-treated controls for western blot analysis. Blots were probed with antibodies against RBL1 and SMAD4, and their protein levels were measured relative to GAPDH. We found that forced overexpression of miR-888 resulted in decreased protein levels for both RBL1 and SMAD4 in PC3-N prostate cancer cells compared with the controls (Fig. 5C).

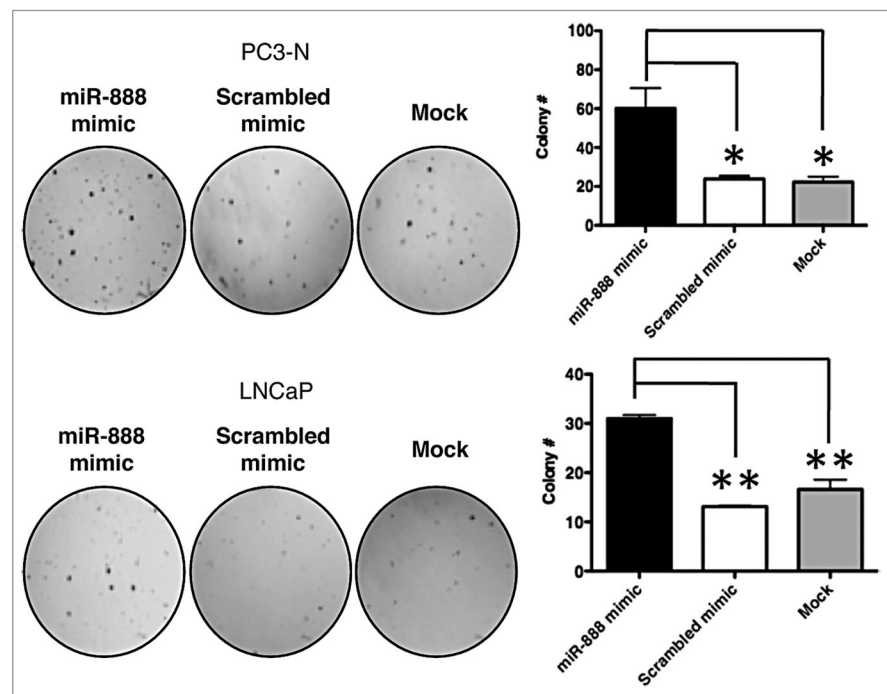


**Figure 4.** miR-888 increased colony formation in PC3-N and LNCaP prostate cancer cells. Anchorage-independent growth in soft agar of PC3-N cells (top panel) and LNCaP cells (bottom panel) was increased in cells treated with miR-888 mimic (50 nM) compared with cells treated with a scrambled mimic (50 nM) or mock-treated cells. Colonies were grown for 14 d, stained with 0.005% crystal violet, and counted. Each graph represents 2 independent trials performed at least in duplicate and error bars show SD \**P*, 0.05, \*\**P* < 0.01; *P* values obtained by 1-way ANOVA with a Tukey post-test.

## Discussion

We have characterized miR-888 as a novel prostate cancer-associated miRNA that correlates with disease status and shares functional features of an oncogenic factor in the prostate. The extent of miRNA

misregulation in human prostate cancer has only recently been appreciated. Little is understood regarding how changes in miRNA expression functionally contribute to the progression of prostate cancer to aggressive and metastatic disease. This is significant, since metastatic prostate disease remains an incurable, lethal form of prostate cancer that would benefit from the development of small RNA diagnostics and therapeutic tools in the clinic. In this study, we screened for miRNAs that correlated with aggressive prostate cancer by comparing expression profiles in 2 established syngeneic prostate cancer PC3 sublines, PC3-ML and PC3-N, that differed in their metastatic potential.

We noted that miR-888 and miR-891a, which reside in the same miRNA cluster on human chromosome X, were 2 of the most differentially expressed miRNAs enriched in aggressive PC3-ML compared with non-invasive PC3-N cells.

We focused on miR-888 in the prostate, since increased expression of this miRNA correlated with hormone insensitivity in cancer cell lines, malignancy in primary prostate tissues from prostate cancer patients, and high-grade forms of prostate disease when analyzing EPS urine specimens. Our in vitro work indicated a functional role for miR-888 in prostate cancer progression to promote proliferation, migration, and colony formation using both

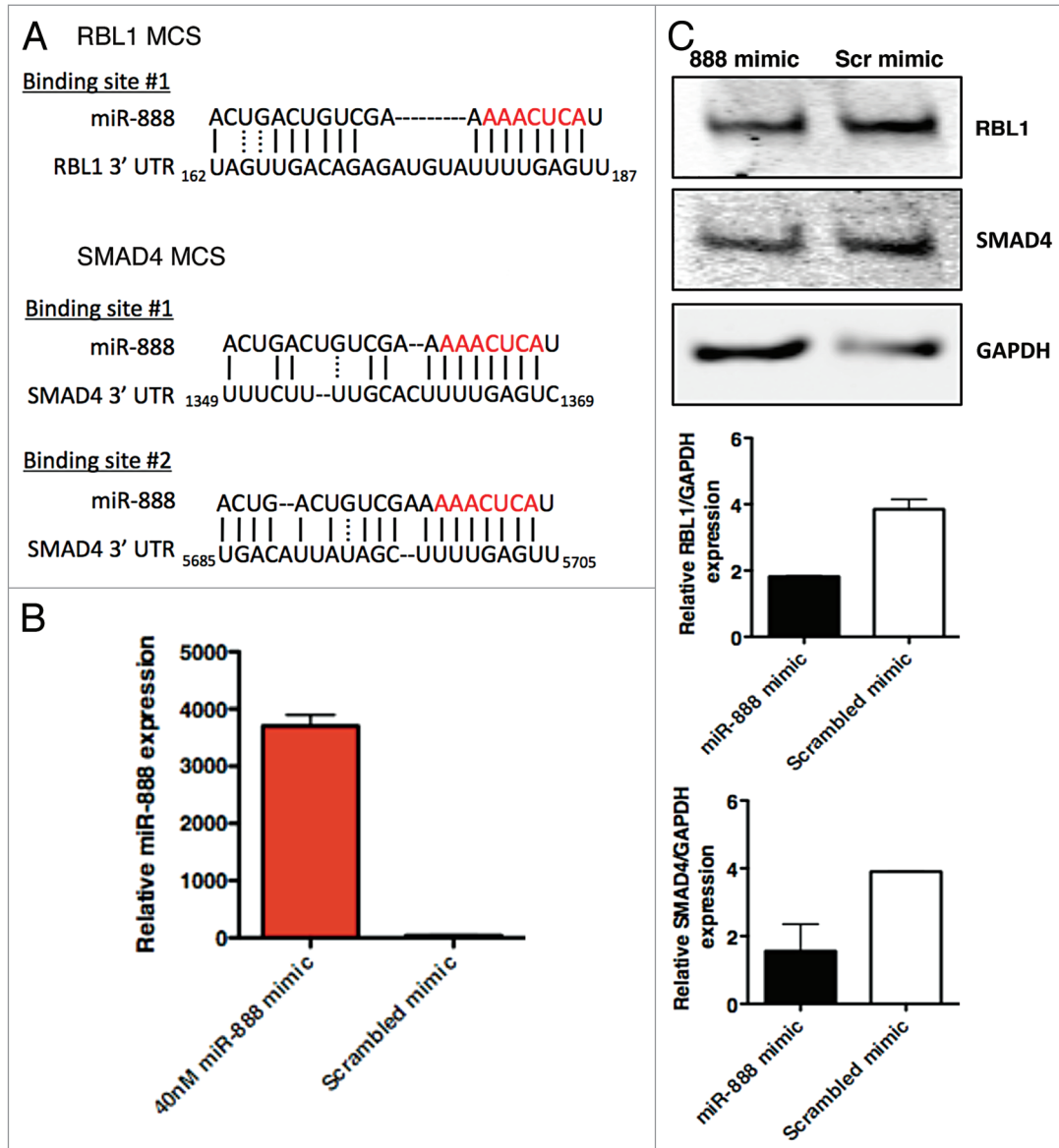


**Figure 5.** Overexpression of miR-888 in human prostate cancer cells decreased RBL1 and SMAD4 protein levels. (A) Top, human RBL1 possesses one predicted miRNA complementary binding site (MCS) for miR-888 in its 3' UTR. Seed region for miR-888 shown in red, dashed line indicates predicted bulge in the RBL1 3' UTR interaction. Bottom, human SMAD4 has 2 predicted binding sites in its 3' UTR for miR-888 (B) Increased miR-888 levels measured using qRT-PCR in PC3-N cells treated with miR-888 mimic (40 nM) compared with scrambled mimic controls (40 nM) 24 h post-transfection. Levels shown are relative to mock-treated cells. (C) Western blot analysis for RBL1 (120 kDa), SMAD4 (61 kDa), and GAPDH1 (37 kDa) expression in PC3-N cells 24 h after transfection with either miR-888 mimic (40 nM) or scrambled mimic controls (40 nM). GAPDH was used as a loading control (note that the scrambled mimic lane was underloaded). Quantitation was done on the Odyssey (Li-Cor). Bar graphs show results from 2 independent trials for RBL1 and SMAD4 detection. Error bars show standard deviation (SD).

PC3 and LNCaP human prostate cancer cell lines that differed in their metastatic status and response to androgens. In the clinic, castration as well as androgen receptor antagonists are widely used to treat prostate cancer and curb tumor growth. However, as the cancer progresses, prostate tumor cells develop resistance to hormonal deprivation therapies. New drugs such as Alpharadin (radium-223 chloride) and Enzalutamide increase survival in patients with castration-resistant prostate cancer by 3–5 mo, not years, reflecting the need for better treatment options for metastatic disease. Our work in PC3-derived cells (representing advanced prostate cancer and sharing features with prostatic small cell neuroendocrine cells<sup>65</sup>) showed that inactivation of miR-888 in PC3-ML cells via miRNA inhibitor treatment resulted in decreased cell growth and migration. These results underscore the potential of miR-888 as a powerful diagnostic tool to detect patients at higher risk earlier during the course of their disease as well as a novel and much-needed therapeutic target to treat androgen-sensitive as well as castration-resistant prostate cancer.

Before this work, no functional role for miR-888 had been defined in the prostate or any other tissues. The miR-888 miRNA belongs to a cluster of 7 miRNA genes (hsa-miR-892c, hsa-miR-890, hsa-miR-888, hsa-miR-892a, hsa-miR-892b, and hsa-miR-891b) residing within a ~34-kb region on the minus strand of chromosome X (Xq27.3) (Fig. 1A). Analysis of the miR-888 cluster indicates that the genomic organization of these 7 miRNAs is highly conserved in primates (humans, chimpanzees, orangutans, and rhesus macaque) but no other mammals.<sup>41</sup> miR-888 and its related miR-890/892a/892b/892c members belong to the mammalian-conserved miR-743 miRNA family and show little sequence homology to the primate-specific miR-891 family members miR-891a and miR-891b. The miR-888 cluster was initially identified via small RNA sequencing in human epididymis tissue, an organ important for male fertility.<sup>40,42,66</sup> miR-888 is expressed consistently throughout the human epididymis, unlike its clustered members miR-890/892a/892b/891a/891b, which are expressed more robustly in the corpus and cauda regions of this organ.<sup>42</sup> These findings imply a role for the miR-888 cluster in the development and/or physiology of the epididymis.

miR-888 misexpression has recently been reported in human cancers. miR-888 is dysregulated in a subset of renal cell carcinomas (RCC). miRNA signatures were used to differentiate histological subtypes of renal cell carcinoma and miR-888 was more highly expressed in chromophobe renal cell carcinomas (chRCC) compared with normal renal tissue or other RCC subtypes.<sup>67</sup> This work also found that 10–15% of papillary renal cell carcinomas showed abnormalities within a locus containing miR-888 on chromosome X.<sup>67</sup> miR-888 has loosely been linked to ovarian cancer, an infrequent somatic mutation mapping within the miR-888 hairpin was identified in a primary epithelial ovarian tumor.<sup>68</sup> Furthermore, miR-888 was isolated out of >600 miRNAs profiled and was one of the most overexpressed small RNAs in endometrial cancers.<sup>69</sup> miR-888 was observed to be particularly upregulated in malignant mixed müllerian tumors (Drs A Hovey and K Leslie, University of Iowa, Department of Obstetrics and Gynecology; personal communication), which is

an extremely aggressive form of this disease with poor patient prognosis. Functional studies for miR-888 in endometrial cancers have not been performed. However, the progesterone receptor (PR) is a predicted target for miR-888—the loss of which is commonly observed in endometrial tumors.<sup>69</sup>

The link between miR-888 and cancer, particularly aggressive endometrial cancer, is striking in light of our own work indicating that higher levels of miR-888 correlate with aggressive forms of prostate cancer. These results are consistent with the notion that miR-888 plays an oncogenic role. However, miR-888 activities are likely not limited to the urologic and reproductive organs. Wang et al. reported that upregulation of miR-888 was associated with differentiation of monocytes.<sup>70</sup> Therefore, although this miRNA was first defined as an epididymis-specific factor, miR-888 likely plays a larger role in cellular development and differentiation processes in multiple organ systems.

We also identified candidate targets for miR-888 using the bioinformatic algorithm TargetScan that are associated with prostate cancer and tumor progression. Our *in vitro* studies indicated that protein levels for the tumor suppressors RBL1 and SMAD4 are negatively modulated by miR-888 in prostate cancer cells. RBL1, belongs to the retinoblastoma (RB) family and functions to block G<sub>1</sub>-S phase cell cycle progression by binding and inhibiting the E2F transcription factors. Decreased expression of RBL1 is associated with the progression of prostate cancers, which reciprocally correlates with our studies showing increased miR-888 in prostate cancer specimens.<sup>71</sup> Interestingly, a negative correlation between miR-888 and RBL1 expression was also noted in differentiated monocytes.<sup>70</sup> The second predicted miR-888 target, SMAD4, is a central intracellular signaling protein that in association with receptor-regulated SMADs, acts as a transducer of the TGF- $\beta$ /BMP ligands to regulate cellular growth and differentiation. Unlike pancreatic and gastroenterological cancers, loss of SMAD4 in prostate cancer is not required for tumor initiation, but rather is considered a later event that relies on the combined loss of factors such as PTEN for the progression of cancer to more aggressive and metastatic disease.<sup>64,72</sup> Our results indicated that elevated levels of miR-888 correlated with prostate cancer progression and, thus, miR-888 could potentially promote aggressive prostate disease by inhibiting SMAD4 expression.

Lastly, our work highlights the utility of EPS urine as a discriminating biomarker source for prostate cancer. EPS urine can be obtained non-invasively during a standard urological exam, an advantage in clinical practice, where selection for active surveillance (AS) and monitoring for progression relies heavily on invasive repeat prostate biopsy and frequent PSA testing. These proximal fluids are currently being used to measure the non-coding RNA PCA3 as well as the fusion transcript TMPRSS2-ERG to predict prostate cancer risk. Our work is the first to show that miRNAs such as miR-888 can be reliably profiled in the supernatant component of EPS urine and discriminate for high-grade prostate cancer. To our knowledge, only one study has reported miRNA expression in EPS urine, focusing on the pellet component, and the researchers failed to identify discriminating miRNA biomarkers within their clinical cancer subgroups.<sup>17</sup>



Our work for miR-888, as well as *let-7c* and miR-200b, showed that disease status more closely correlated with the supernatant rather than the pellet fraction of EPS urine. EPS urine supernatant is likely a better biomarker source because of the presence of exosomes in this fraction, which can be purified by high-speed ultra-centrifugation. Exosomes are 50–150-nm-membrane-bound microvesicles actively secreted by many cell types, including tumor cells shown to selectively concentrate and transport miRNAs intercellularly.<sup>73</sup> Going forward, it will be important to validate the utility of measuring miRNA levels in the supernatant (and/or exosomes) vs. pellet EPS urine fractions to discriminate for aggressive prostate cancer on larger patient cohorts and in more defined clinical groups. EPS urine screening could aid clinicians in more accurately risk-stratifying patients, leading to better personalized treatment, i.e., directing those with highest risk of aggressive disease toward multimodal therapies and those with more indolent profiles could more confidently enroll in watchful waiting protocols.

In conclusion, we have identified miR-888 as a novel small RNA that is elevated in cell lines, tissues, and EPS urine from patients with prostate cancer and functions to promote proliferation, migration, and colony formation of prostate cells. It will be challenging to understand how miR-888 acts in a network with other oncogenic and tumor suppressor non-coding RNAs and protein-coding genes to impact the overall etiology of prostate cancer and contribute to the transformation of cancer cells into a more aggressive and metastatic state.

## Materials and Methods

### Cell culture

PC3 (American Type Culture Collection), PC3-ML and PC3-N (gift from Dr M Stearns) were grown in DMEM supplemented with 10% fetal bovine serum and 1% antibiotic-antimycotic (Gibco). LNCaP (American Type Culture Collection) and PacMetUT1 (gift from Dr L deGraffenried) were grown in RPMI-1640 supplemented with 10% fetal bovine serum and 1% antibiotic-antimycotic. RWPE-1 cells were grown in Keratinocyte serum-free media (Gibco) supplemented with 1% antibiotic-antimycotic, 0.05 mg/mL bovine pituitary extract and 5 ng/mL recombinant epidermal growth factor growth factor. All cells were grown at 37 °C with 5% CO<sub>2</sub>.

### miRNA profiling of prostate cancer cell lines

#### *TaqMan low-density arrays*

The expression of 377 miRNAs was profiled for the PC3-derived sublines, PC3-N and PC3-ML, using microfluidic miRNA TaqMan-based qRT-PCR low-density arrays (Human MicroRNA A Card v2.0, Applied Biosystems, Life Technologies). Five hundred nanograms of total RNA from each cell line was isolated (Ambion mirVana miRNA Isolation Kit, Life Technologies) and reverse transcribed using the stem-loop based Megaplex RT Primers, Human Pool A, and the resulting product was loaded together with TaqMan Universal PCR Master Mix, No AmpErase UNG onto a 384-well TaqMan MicroRNA Assay microfluidic plate. The qRT-PCR measurements were performed on an Applied BioSystems 7900HT thermocycler. These studies

were performed in duplicate for each cell line and normalized to mammalian snoRNA U6 using *Arabidopsis thaliana* Ath-miR-159a as a negative control. miRNA expression profiles were compared between the PC3-ML and PC3-N cell lines using the  $\Delta\Delta C_t$  method.

#### *TaqMan miRNA assays*

miRNA expression was verified using individual TaqMan-based qRT-PCR assays (Applied Biosystems, Life Technologies) on total RNA obtained via the Ambion mirVana miRNA Isolation Kit (Life Technologies) from the prostate cell lines PC3-N and PC3-ML sublines, the PC3 (parental), LNCaP, PacMetUT1, and RWPE-1 cell lines (a complete summary of TaqMan Assays used for miRNA detection is found in Table S3). Briefly, reverse transcription reactions were performed in triplicate on 35 ng of total RNA with the TaqMan MicroRNA Reverse Transcription Kit and miRNA-specific stem-loop primers (Applied Biosystems, Life Technologies). Singleplex reactions were performed in 15  $\mu$ L and contained: 0.15  $\mu$ L 100 mM dNTP, 1.00  $\mu$ L multiscribe reverse transcriptase (50 U/ $\mu$ L), 0.19  $\mu$ L RNase inhibitor (20 units/ $\mu$ L), 1.50  $\mu$ L 10 $\times$  reverse transcription buffer, 7  $\mu$ L (5 ng/ $\mu$ L) total RNA, 2.16  $\mu$ L nuclease-free water, and 3.00  $\mu$ L miRNA stem-loop primer. Multiplex reactions for 8 different genes were performed in 60  $\mu$ L and contained: 0.60  $\mu$ L 100 mM dNTP, 4.00  $\mu$ L multiscribe reverse transcriptase (50 U/ $\mu$ L), 0.76  $\mu$ L RNase inhibitor (20 U/ $\mu$ L), 6.00  $\mu$ L 10 $\times$  reverse transcription buffer, 17.64  $\mu$ L nuclease-free water, 7  $\mu$ L (5 ng/ $\mu$ L) total RNA, and 24  $\mu$ L miRNA stem-loop primers (3.00  $\mu$ L for each miRNA, 8 genes total). Reverse transcription reactions were performed using an Applied Biosystems Veriti 96-well thermal cycler (Life Technologies) under the following conditions: 16 °C for 30 min, 42 °C for 30 min, 85 °C for 5 min. Twenty microliters of the qRT-PCR reactions were prepared in triplicate, each reaction containing 1  $\mu$ L TaqMan real-time miRNA assay, 4.5  $\mu$ L reverse transcribed RNA, 10  $\mu$ L TaqMan 2 $\times$  Universal PCR Master Mix, No AmpErase UNG, and 4.5  $\mu$ L nuclease-free water. Real-time PCR reactions were run under the following conditions: 95 °C for 10 min, 40 cycles of 95 °C for 15 s and 60 °C for 1 min. miRNA expression was normalized to snoRNA RNU48. Relative fold-change in miRNA expression was calculated comparing each cancer cell line vs. RWPE-1 cells using the  $\Delta\Delta C_t$  method.

#### **EPS urine profiling for miRNA expression**

EPS urine specimens were collected by a clinician via urine capture following gentle massage of the prostate gland during a digital rectal exam (DRE) just prior to the original diagnostic biopsy. Massage of the prostate consisted of three strokes on each side of the median sulcus, stimulating the release and movement of prostate fluids and detached epithelial cells directly into the urethra. Specimens were required to have at least 20  $\mu$ g/mL PSA values as a means to standardize the efficiency of the prostate massage to push proximal secretions into the urethra. Nine milliliters of each specimen was centrifuged at 2500 rpm for 15 min to separate the EPS urine into supernatant and pellet fractions. The de-identified EPS urine specimens were obtained from the biorepository at the Leroy T. Canoles Jr. Cancer Research Center under protocols approved by the Eastern Virginia Medical

School (EVMS) Institutional Review Board (IRB) and in accordance with NIH guidelines and HIPAA regulations. EPS urine specimens were grouped based on clinical grade: non-cancer (24 patients), cancer (Gleason 6-7, 25 patients; Gleason 8, one patient), and high-grade cancer (Gleason 9-10, 6 patients).

#### *For EPS urine supernatant fractions*

Total RNA was isolated from 500  $\mu$ L of EPS urine supernatant using a modified protocol for the miRNeasy Mini Kit (Qiagen). Since no standard normalization procedure exists for measuring miRNA expression in body fluids that possess low concentrations of RNA, *C. elegans* miRNA miR-39 (sharing no homology to human miRNAs) was spiked into the EPS urine supernatant fractions prior to RNA isolation, as similarly used for small RNA profiling in blood.<sup>13</sup> (Optical density [OD] measurements and normalization with cellular-derived RNA species such as RNU48 are inappropriate for this application.) Specifically, 700  $\mu$ L of QIAzol Lysis Reagent was added to the EPS sample and incubated for 5 min at room temperature. 5  $\mu$ L of 50 fMol *C. elegans* miRNA miR-39 was spiked into each sample. 140  $\mu$ L of chloroform was added and mixed briefly. The sample was then incubated at room temperature for 3 min and centrifuged for 15 min at 12 100 RPM at 4 °C. The upper aqueous layer was extracted and 1.5 volumes (1200  $\mu$ L) of 100% ethanol was added and mixed. The sample was then loaded onto the miRNeasy mini column and the remaining protocol was followed. Total RNA was eluted with 50  $\mu$ L of nuclease free water. For qRT-PCR reactions using TaqMan-based miRNA assays, 9.16  $\mu$ L of eluted total RNA was used for each singleplex or multiplex reverse transcription reaction as described in the *TaqMan Assay* section. miRNA expression for the EPS urine supernatant was normalized to cel-miR-39 expression and average fold-differences between cancer and non-cancer expression levels were obtained using the  $\Delta\Delta$ Ct method.

#### *For EPS urine pellets*

Total RNA was isolated using the Ambion mirVana miRNA Isolation Kit (Life Technologies) according to the manufacturer's instructions. Fifty nanograms of total RNA was reverse transcribed using the TaqMan MicroRNA Reverse Transcription Kit and TaqMan human miRNA assays (Applied Biosystems, Life Technologies). Singleplex and multiplex reactions were performed as described. miRNA expression for the pellets was normalized using the mean of two reference snoRNAs (RNU44 and RNU48). To determine relative miR-888 expression in individual EPS urine pellets from 20 prostate cancer patients, the average delta Ct for miR-888 expression in EPS urine pellets from 11 non-cancer patients was calculated. Average fold-differences between cancer and non-cancer expression levels were obtained using the  $\Delta\Delta$ Ct method.

#### **miRNA expression studies on clinical FFPE prostate specimens**

miRNA expression profiles using de-identified FFPE (Formalin-Fixed, Paraffin-Embedded) primary prostate tissue specimens from a cohort of prostate cancer patients diagnosed with insignificant disease (tumor size  $\leq$  0.5 mL, stage  $\leq$  T2, Gleason  $\leq$  6), significant disease (tumor confined to the prostate, stage T2, any Gleason, 5 y follow-up with no metastasis

or biochemical recurrence), and metastatic disease (confirmed distant metastasis) as well as non-prostate cancer patients. These specimens were obtained from the biorepository at the Leroy T. Canoles Jr. Cancer Research Center under protocols approved by the EVMS Institutional Review Board and in accordance with NIH guidelines and HIPAA regulations. For these experiments, total RNA was isolated from manual scrapings of FFPE prostate tumor or normal tissue sections (as identified by a pathologist) with roughly 20 microns thickness using the Ambion RecoverAll Total Nucleic Acid Isolation Kit (Life Technologies). Multiplex stem-loop reverse transcription reactions were performed using 25 ng of total RNA and TaqMan qRT-PCR was done in triplicate as described previously. miRNA values were normalized through expression of snoRNA RNU48, and average fold-differences between cancerous and non-cancer expression levels were obtained using the  $\Delta\Delta$ Ct method.

#### **miRNA transfections in cell culture**

PC3-derived cell lines or LNCaP cells were reverse transfected in triplicate with Ambion siPORT NeoFX Transfection Agent (Life Technologies) and 40 nM or 50 nM hsa-miR-888 Ambion Pre-miR miRNA Precursor (AM17100 Product ID: PM12400, Life Technologies) or Pre-miR miRNA Precursor Negative Control (AM17110, Life Technologies). For miR-888 inhibition experiments, cells were transfected with Lipofectamine RNAi Max Reagent (Life Technologies) and 50 nM hsa-miR-888 Dharmacon miRIDIAN MicroRNA Hairpin Inhibitor (IH-301228-02, Thermo Scientific) or scrambled Dharmacon miRIDIAN MicroRNA Hairpin Inhibitor Negative Control #1 (IN-001005-01-05, Thermo Scientific). Mock-transfected cells were only treated with the respective transfection reagents.

#### **Cell proliferation WST-1 assay**

Transfected cells were plated at a density of 2000 cells/100  $\mu$ L (80 mL cells in DMEM + 20 mL siPORT + 50 nM miRNA mimic or 90 mL cells in DMEM + 10 mL Lipofectamine RNAimax + 50 nM miRNA inhibitor) in a flat-bottom 96-well plate and allowed to incubate overnight before adding fresh DMEM medium. Four hours prior to the 24-, 48-, and 72-h time points, 10  $\mu$ L of WST-1 reagent (Roche Applied Science) was added to each well. Formazan conversion was then measured with a microplate reader (Biotek Synergy) at a test wavelength of 450 nm and reference wavelength of 620 nm. Values from blank wells (DMEM + WST-1 reagent) were subtracted from all experimental wells.

#### **Cell migration scratch assay**

Prostate cancer cells transfected with 50 nM of miR-888 mimic or scrambled controls were plated at a density of  $1 \times 10^6$  cells/well in a 6-well plate. Scratches were made with a p200 pipette tip 24 h post-transfection. Each well was then rinsed 5 times with PBS to clear floating cells from scratches, and 3 mL of 3% fetal bovine serum (FBS), 1% antibiotic-antimycotic DMEM was added to each well. Images were taken at time 0, immediately following the scratch and 24 h later with a Zeiss Axio Observer.A1 inverted microscope (10 $\times$  objective) and an Axiocam MRm camera with a 0.63 $\times$  adaptor. Results were quantified by determining the percent scratch closed; (initial scratch width-final scratch width)/initial scratch width  $\times$  100%.

### Boyden chamber transwell migration assays

Prostate cancer cells transfected with 50 nM of miR-888 mimic or scrambled controls were added to the top of a Boyden chamber insert (BD BioCoat Inserts, BDBiosciences) at a density of  $6 \times 10^5$  cells/well in a 6-well plate. Twenty-four hours post-transfection, cells that traversed across the polycarbonated insert toward the chemoattractant (10% FBS) were methanol-fixed and stained with 1% crystal violet. Wells were destained in 10% acetic acid and 30% methanol. Results were quantified in triplicate for each well from 100  $\mu$ L of destain solution using 96-well plates and measured in a spectrophotometer (Synergy HT, BioTek) at 595-nm wavelength.

### Apoptosis assay-flow cytometry

Transfected cells were plated at a density of  $2.4 \times 10^5$  cells/well in a 6-well plate and incubated for 24 h. Cell pellets were harvested from each well and stained with Annexin V and 7AAD according to the General Annexin V Staining Procedure from Becton Dickinson Sciences. Immediately following staining, cells were analyzed by flow cytometry using a Cytex DXP 8 color 488/637/407 (Cytex Development Inc) upgraded FACSCalibur (Becton Dickinson) and FlowJo software version 7.6 (Treestar).

### Western blot analysis

Protein extracts were prepared by lysing cells 24 h post-transfection in RIPA buffer (50 mM Tris-Cl pH 8, 150 mM NaCl, 5 mM MgCl<sub>2</sub>, 1% TritonX-100, 0.5% Na-deoxycholate, 0.1% SDS) with protease inhibitors and resolved on 4–15% Tris-HCL gels (Ready Gel, BioRad) for western blot analysis. Immobilon-FL membranes (Millipore) were blocked with Odyssey Blocking Buffer in 1 $\times$  phosphate-buffered saline (1 $\times$  PBS) for 1 h and probed overnight in Odyssey Blocking Buffer, 1 $\times$  PBS, and 0.1% Tween-20 at 4 °C with primary antibodies against RBL1 (1:200, Santa Cruz sc-318), SMAD4 (1:500, Santa Cruz sc-7154), and

GAPDH (1:2000, Abcam ab-8245). Blots were washed in PBST and then probed in Odyssey Blocking Buffer, 1 $\times$  PBS, 0.1% Tween-20 and 0.01% SDS at room temperature with secondary goat anti-mouse (1:5000–1:10 000) or goat anti-rabbit (1:20 000) antibodies (Li-Cor). Protein expression was quantitated relative to GAPDH levels using an Odyssey scanner and software (Li-Cor).

### Disclosure of Potential Conflicts of Interest

No potential conflicts of interest were disclosed.

### Acknowledgments

Amy Tang, Minglei Bian, Matthew Butcher, Tanya Burch and Xin (Cindy) Guo provided technical advice for the in vitro assays; Mary Ann Clements and Elizabeth Smith assisted in retrieval and sectioning of FFPE specimens obtained from the biorepository at the EVMS Leroy T. Canoles Jr. Cancer Center; Sydney Radding and Patricia Railing participated in total RNA isolation of FFPE specimens; and Brain Main coordinated specimen clinical data retrieval for these studies. The PC3-derived sublines, PC3-N and PC3-ML, were kindly provided by Mark Stearns (Drexel University College of Medicine) and the PacMetUT1 cell line was a gift from Linda deGraffenried (University of Texas Health Science Center San Antonio). AE-K was supported by an ARRA grant from the National Institute of Health (RO3 CA139547-01) and start-up funds from Eastern Virginia Medical School. AE-K and RRD were supported by a grant from the National Cancer Institute (R21 CA137704-01).

### Supplemental Materials

Supplemental materials may be found here: [www.landesbioscience.com/journals/cc/article/26984](http://www.landesbioscience.com/journals/cc/article/26984)

### References

1. Lilja H, Ulmert D, Vickers AJ. Prostate-specific antigen and prostate cancer: prediction, detection and monitoring. *Nat Rev Cancer* 2008; 8:268-78; PMID:18337732; <http://dx.doi.org/10.1038/nrc2351>
2. Schröder FH. Review of diagnostic markers for prostate cancer. *Recent Results Cancer Res* 2009; 181:173-82; PMID:19213567; [http://dx.doi.org/10.1007/978-3-540-69297-3\\_16](http://dx.doi.org/10.1007/978-3-540-69297-3_16)
3. Lin K, Lipsitz R, Miller T, Janakiraman S; U.S. Preventive Services Task Force. Benefits and harms of prostate-specific antigen screening for prostate cancer: an evidence update for the U.S. Preventive Services Task Force. *Ann Intern Med* 2008; 149:192-9; PMID:18678846; <http://dx.doi.org/10.7326/0003-4819-149-3-200808050-00009>
4. Moyer VA; U.S. Preventive Services Task Force. Screening for prostate cancer: U.S. Preventive Services Task Force recommendation statement. *Ann Intern Med* 2012; 157:120-34; PMID:22801674; <http://dx.doi.org/10.7326/0003-4819-157-2-201207170-00459>
5. Maugeri-Saccà M, Coppola V, Bonci D, De Maria R. MicroRNAs and prostate cancer: from pre-clinical research to translational oncology. *Cancer J* 2012; 18:253-61; PMID:22647362; <http://dx.doi.org/10.1097/PPO.0b013e318258b5b6>
6. Griffiths-Jones S, Saini HK, van Dongen S, Enright AJ. miRBase: tools for microRNA genomics. *Nucleic Acids Res* 2008; 36:D154-8; PMID:17991681; <http://dx.doi.org/10.1093/nar/gkm952>
7. Calin GA, Croce CM. MicroRNA signatures in human cancers. *Nat Rev Cancer* 2006; 6:857-66; PMID:17060945; <http://dx.doi.org/10.1038/nrc1997>
8. Esquela-Kerscher A, Slack FJ. Oncomirs - microRNAs with a role in cancer. *Nat Rev Cancer* 2006; 6:259-69; PMID:16557279; <http://dx.doi.org/10.1038/nrc1840>
9. Bartel DP. MicroRNAs: genomics, biogenesis, mechanism, and function. *Cell* 2004; 116:281-97; PMID:14744438; [http://dx.doi.org/10.1016/S0092-8674\(04\)00045-5](http://dx.doi.org/10.1016/S0092-8674(04)00045-5)
10. Filipowicz W, Bhattacharyya SN, Sonenberg N. Mechanisms of post-transcriptional regulation by microRNAs: are the answers in sight? *Nat Rev Genet* 2008; 9:102-14; PMID:18197166; <http://dx.doi.org/10.1038/nrg2290>
11. Ozen M, Creighton CJ, Ozdemir M, Ittmann M. Widespread deregulation of microRNA expression in human prostate cancer. *Oncogene* 2008; 27:1788-93; PMID:17891175; <http://dx.doi.org/10.1038/sj.onc.1210809>
12. Gandellini P, Folini M, Zaffaroni N. Towards the definition of prostate cancer-related microRNAs: where are we now? *Trends Mol Med* 2009; 15:381-90; PMID:19716766; <http://dx.doi.org/10.1016/j.molmed.2009.07.004>
13. Mitchell PS, Parkin RK, Kroh EM, Fritz BR, Wyman SK, Pogosova-Agadjanyan EL, Peterson A, Noteboom J, O'Brian KC, Allen A, et al. Circulating microRNAs as stable blood-based markers for cancer detection. *Proc Natl Acad Sci U S A* 2008; 105:10513-8; PMID:18663219; <http://dx.doi.org/10.1073/pnas.0804549105>
14. Weber JA, Baxter DH, Zhang S, Huang DY, Huang KH, Lee MJ, Galas DJ, Wang K. The microRNA spectrum in 12 body fluids. *Clin Chem* 2010; 56:1733-41; PMID:20847327; <http://dx.doi.org/10.1373/clinchem.2010.147405>
15. Lawrie CH, Gal S, Dunlop HM, Pushkaran B, Liggins AP, Pulford K, Banham AH, Pezzella F, Boulwood J, Wainscoat JS, et al. Detection of elevated levels of tumour-associated microRNAs in serum of patients with diffuse large B-cell lymphoma. *Br J Haematol* 2008; 141:672-5; PMID:18318758; <http://dx.doi.org/10.1111/j.1365-2141.2008.07077.x>
16. Park NJ, Zhou H, Elashoff D, Henson BS, Kastratovic DA, Abemayor E, Wong DT. Salivary microRNA: discovery, characterization, and clinical utility for oral cancer detection. *Clin Cancer Res* 2009; 15:5473-7; PMID:19706812; <http://dx.doi.org/10.1158/1078-0432.CCR-09-0736>
17. Bryant RJ, Pawlowski T, Catto JW, Marsden G, Vessella RL, Rhee B, Kuslich C, Visakorpi T, Hamdy FC. Changes in circulating microRNA levels associated with prostate cancer. *Br J Cancer* 2012; 106:768-74; PMID:22240788; <http://dx.doi.org/10.1038/bjc.2011.595>

18. Tsujiura M, Ichikawa D, Komatsu S, Shiozaki A, Takeshita H, Kosuga T, Konishi H, Morimura R, Deguchi K, Fujiwara H, et al. Circulating microRNAs in plasma of patients with gastric cancers. *Br J Cancer* 2010; 102:1174-9; PMID:20234369; <http://dx.doi.org/10.1038/sj.bjc.6605608>
19. Nadiminty N, Tummala R, Lou W, Zhu Y, Zhang J, Chen X, eVere White RW, Kung HJ, Evans CP, Gao AC. MicroRNA *let-7c* suppresses androgen receptor expression and activity via regulation of *Myc* expression in prostate cancer cells. *J Biol Chem* 2012; 287:1527-37; PMID:22128178; <http://dx.doi.org/10.1074/jbc.M111.278705>
20. Nadiminty N, Tummala R, Lou W, Zhu Y, Shi XB, Zou JX, Chen H, Zhang J, Chen X, Luo J, et al. MicroRNA *let-7c* is downregulated in prostate cancer and suppresses prostate cancer growth. *PLoS One* 2012; 7:e32832; PMID:22479342; <http://dx.doi.org/10.1371/journal.pone.0032832>
21. Bonci D, Coppola V, Musumeci M, Addario A, Giuffrida R, Memeo L, D'Urso L, Pagliuca A, Biffoni M, Labbaye C, et al. The miR-15a-miR-16-1 cluster controls prostate cancer by targeting multiple oncogenic activities. *Nat Med* 2008; 14:1271-7; PMID:18931683; <http://dx.doi.org/10.1038/nm.1880>
22. Kong D, Li Y, Wang Z, Banerjee S, Ahmad A, Kim HR, Sarkar FH. miR-200 regulates PDGF-D-mediated epithelial-mesenchymal transition, adhesion, and invasion of prostate cancer cells. *Stem Cells* 2009; 27:1712-21; PMID:19544444; <http://dx.doi.org/10.1002/stem.101>
23. Vrba L, Jensen TJ, Garbe JC, Heimark RL, Cress AE, Dickinson S, Stampfer MR, Futscher BW. Role for DNA methylation in the regulation of miR-200c and miR-141 expression in normal and cancer cells. *PLoS One* 2010; 5:e8697; PMID:20084174; <http://dx.doi.org/10.1371/journal.pone.0008697>
24. Vallejo DM, Caparros E, Dominguez M. Targeting Notch signalling by the conserved miR-8/200 microRNA family in development and cancer cells. *EMBO J* 2011; 30:756-69; PMID:21224847; <http://dx.doi.org/10.1038/emboj.2010.358>
25. Sun D, Lee YS, Malhotra A, Kim HK, Maticic M, Evans C, Jensen RV, Moskaluk CA, Dutta A. miR-99 family of MicroRNAs suppresses the expression of prostate-specific antigen and prostate cancer cell proliferation. *Cancer Res* 2011; 71:1313-24; PMID:21212412; <http://dx.doi.org/10.1158/0008-5472.CAN-10-1031>
26. Varambally S, Cao Q, Mani RS, Shankar S, Wang X, Ateeq B, Laxman B, Cao X, Jing X, Ramnarayanan K, et al. Genomic loss of microRNA-101 leads to overexpression of histone methyltransferase EZH2 in cancer. *Science* 2008; 322:1695-9; PMID:19008416; <http://dx.doi.org/10.1126/science.1165395>
27. Cao P, Deng Z, Wan M, Huang W, Cramer SD, Xu J, Lei M, Sui G. MicroRNA-101 negatively regulates Ezh2 and its expression is modulated by androgen receptor and HIF-1alpha/HIF-1beta. *Mol Cancer* 2010; 9:108; PMID:20478051; <http://dx.doi.org/10.1186/1476-4598-9-108>
28. Noonan EJ, Place RF, Pookot D, Basak S, Whitson JM, Hirata H, Giardina C, Dahiya R. miR-449a targets HDAC-1 and induces growth arrest in prostate cancer. *Oncogene* 2009; 28:1714-24; PMID:19252524; <http://dx.doi.org/10.1038/onc.2009.19>
29. Coppola V, De Maria R, Bonci D. MicroRNAs and prostate cancer. *Endocr Relat Cancer* 2010; 17:F1-17; PMID:19779034; <http://dx.doi.org/10.1677/ERC-09-0172>
30. Gordanpour A, Nam RK, Sugar L, Seth A. MicroRNAs in prostate cancer: from biomarkers to molecularly-based therapeutics. *Prostate Cancer Prostatic Dis* 2012; 15:314-9; PMID:22333688; <http://dx.doi.org/10.1038/pcan.2012.3>
31. Poliseno L, Salmena L, Riccardi L, Fornari A, Song MS, Hobbs RM, Sportoletti P, Varmeh S, Egia A, Fedele G, et al. Identification of the miR-106b-25 microRNA cluster as a proto-oncogenic PTEN-targeting intron that cooperates with its host gene MCM7 in transformation. *Sci Signal* 2010; 3:ra29; PMID:20388916; <http://dx.doi.org/10.1126/scisignal.2000594>
32. Liu C, Kelnar K, Liu B, Chen X, Calhoun-Davis T, Li H, Patrawala L, Yan H, Jeter C, Honorio S, et al. The microRNA miR-34a inhibits prostate cancer stem cells and metastasis by directly repressing CD44. *Nat Med* 2011; 17:211-5; PMID:21240262; <http://dx.doi.org/10.1038/nm.2284>
33. Saini S, Majid S, Shahryari V, Arora S, Yamamura S, Chang I, Zaman MS, Deng G, Tanaka Y, Dahiya R. miRNA-708 control of CD44(+) prostate cancer-initiating cells. *Cancer Res* 2012; 72:3618-30; PMID:22552290; <http://dx.doi.org/10.1158/0008-5472.CAN-12-0540>
34. Ru P, Steele R, Newhall P, Phillips NJ, Toth K, Ray RB. miRNA-29b suppresses prostate cancer metastasis by regulating epithelial-mesenchymal transition signaling. *Mol Cancer Ther* 2012; 11:1166-73; PMID:22402125; <http://dx.doi.org/10.1158/1535-7163.MCT-12-0100>
35. Wang M, Stearns ME. Isolation and characterization of PC-3 human prostatic tumor sublines which preferentially metastasize to select organs in S.C.I.D. mice. *Differentiation* 1991; 48:115-25; PMID:1773917; <http://dx.doi.org/10.1111/j.1432-0436.1991.tb00250.x>
36. Murata T, Takayama K, Katayama S, Urano T, Horie-Inoue K, Ikeda K, Takahashi S, Kawazu C, Hasegawa A, Ouchi Y, et al. miR-148a is an androgen-responsive microRNA that promotes LNCaP prostate cell growth by repressing its target CAND1 expression. *Prostate Cancer Prostatic Dis* 2010; 13:356-61; PMID:20820187; <http://dx.doi.org/10.1038/pcan.2010.32>
37. Fletcher CE, Dart DA, Sita-Lumsden A, Cheng H, Rennie PS, Bevan CL. Androgen-regulated processing of the oncomir miR-27a, which targets Prohibitin in prostate cancer. *Hum Mol Genet* 2012; 21:3112-27; PMID:22505583; <http://dx.doi.org/10.1093/hmg/ddi139>
38. Galardi S, Mercatelli N, Giorda E, Massalini S, Frajese GV, Ciafrè SA, Farace MG. miR-221 and miR-222 expression affects the proliferation potential of human prostate carcinoma cell lines by targeting p27Kip1. *J Biol Chem* 2007; 282:23716-24; PMID:17569667; <http://dx.doi.org/10.1074/jbc.M701805200>
39. Lee KH, Chen YL, Yeh SD, Hsiao M, Lin JT, Goan YG, Lu PJ. MicroRNA-330 acts as tumor suppressor and induces apoptosis of prostate cancer cells through E2F1-mediated suppression of Akt phosphorylation. *Oncogene* 2009; 28:3360-70; PMID:19597470; <http://dx.doi.org/10.1038/onc.2009.192>
40. Landgraf P, Rusu M, Sheridan R, Sewer A, Iovino N, Aravin A, Pfeffer S, Rice A, Kamphorst AO, Landthaler M, et al. A mammalian microRNA expression atlas based on small RNA library sequencing. *Cell* 2007; 129:1401-14; PMID:17604727; <http://dx.doi.org/10.1016/j.cell.2007.04.040>
41. Li J, Liu Y, Dong D, Zhang Z. Evolution of an X-linked primate-specific micro RNA cluster. *Mol Biol Evol* 2010; 27:671-83; PMID:19933172; <http://dx.doi.org/10.1093/molbev/msp284>
42. Belleannée C, Calvo E, Thimon V, Cyr DG, Légaré C, Garneau L, Sullivan R. Role of microRNAs in controlling gene expression in different segments of the human epididymis. *PLoS One* 2012; 7:e34996; PMID:22511979; <http://dx.doi.org/10.1371/journal.pone.0034996>
43. Bello D, Webber MM, Kleinman HK, Wartinger DD, Rhim JS. Androgen responsive adult human prostatic epithelial cell lines immortalized by human papillomavirus 18. *Carcinogenesis* 1997; 18:1215-23; PMID:9214605; <http://dx.doi.org/10.1093/carcin/18.6.1215>
44. Troyer DA, Tang Y, Bedolla R, Adhvariyu SG, Thompson IM, Abboud-Werner S, Sun LZ, Friedrichs WE, deGraffenried LA. Characterization of PacMetUT1, a recently isolated human prostate cancer cell line. *Prostate* 2008; 68:883-92; PMID:18361412; <http://dx.doi.org/10.1002/pros.20758>
45. Villers AA, McNeal JE, Redwine EA, Freiha FS, Stamey TA. Pathogenesis and biological significance of seminal vesicle invasion in prostatic adenocarcinoma. *J Urol* 1990; 143:1183-7; PMID:2342179
46. Epstein JI, Carmichael M, Walsh PC. Adenocarcinoma of the prostate invading the seminal vesicle: definition and relation of tumor volume, grade and margins of resection to prognosis. *J Urol* 1993; 149:1040-5; PMID:8483205
47. Pierorazio PM, Ross AE, Schaeffer EM, Epstein JI, Han M, Walsh PC, Partin AW. A contemporary analysis of outcomes of adenocarcinoma of the prostate with seminal vesicle invasion (pT3b) after radical prostatectomy. *J Urol* 2011; 185:1691-7; PMID:21419448; <http://dx.doi.org/10.1016/j.juro.2010.12.059>
48. Sapre N, Pedersen J, Hong MK, Harewood L, Peters J, Costello AJ, Hovens CM, Corcoran NM. Re-evaluating the biological significance of seminal vesicle invasion (SVI) in locally advanced prostate cancer. *BJU Int* 2012; 110(Suppl 4):58-63; PMID:23194127; <http://dx.doi.org/10.1111/j.1464-410X.2012.11477.x>
49. Drake RR, Elschenbroich S, Lopez-Perez O, Kim Y, Ignatchenko V, Ignatchenko A, Nyalwidhe JO, Basu G, Wilkins CE, Gjurich B, et al. In-depth proteomic analyses of direct expressed prostatic secretions. *J Proteome Res* 2010; 9:2109-16; PMID:20334419; <http://dx.doi.org/10.1021/pr1001498>
50. Drake RR, White KY, Fuller TW, Igwe E, Clements MA, Nyalwidhe JO, Given RW, Lance RS, Semmes OJ. Clinical collection and protein properties of expressed prostatic secretions as a source for biomarkers of prostatic disease. *J Proteomics* 2009; 72:907-17; PMID:19457353; <http://dx.doi.org/10.1016/j.jprot.2009.01.007>
51. Johnson CD, Esquela-Kerscher A, Stefani G, Byrom M, Kelnar K, Ovcharenko D, Wilson M, Wang X, Shelton J, Shingara J, et al. The *let-7* microRNA represses cell proliferation pathways in human cells. *Cancer Res* 2007; 67:7713-22; PMID:17699775; <http://dx.doi.org/10.1158/0008-5472.CAN-07-1083>
52. Spizzo R, Nicoloso MS, Croce CM, Calin GA. SnapShot: microRNAs in Cancer. *Cell* 2009; 137:586-e1, e1; PMID:19410551; <http://dx.doi.org/10.1016/j.cell.2009.04.040>
53. Esquela-Kerscher A, Trang P, Wiggins JF, Patrawala L, Cheng A, Ford L, Weidhaas JB, Brown D, Bader AG, Slack FJ. The *let-7* microRNA reduces tumor growth in mouse models of lung cancer. *Cell Cycle* 2008; 7:759-64; PMID:18344688; <http://dx.doi.org/10.4161/cc.7.6.5834>

54. Porkka KP, Pfeiffer MJ, Waltering KK, Vessella RL, Tammela TL, Visakorpi T. MicroRNA expression profiling in prostate cancer. *Cancer Res* 2007; 67:6130-5; PMID:17616669; <http://dx.doi.org/10.1158/0008-5472.CAN-07-0533>
55. Chen C, Bhalala HV, Vessella RL, Dong JT. KLF5 is frequently deleted and down-regulated but rarely mutated in prostate cancer. *Prostate* 2003; 55:81-8; PMID:12661032; <http://dx.doi.org/10.1002/pros.10205>
56. Eeles RA, Kote-Jarai Z, Giles GG, Olama AA, Guy M, Jugurnauth SK, Mulholland S, Leongamornlert DA, Edwards SM, Morrison J, et al.; UK Genetic Prostate Cancer Study Collaborators; British Association of Urological Surgeons' Section of Oncology; UK ProtecT Study Collaborators. Multiple newly identified loci associated with prostate cancer susceptibility. *Nat Genet* 2008; 40:316-21; PMID:18264097; <http://dx.doi.org/10.1038/ng.90>
57. Ghosh AK, Steele R, Ray RB. c-myc Promoter-binding protein 1 (MBP-1) regulates prostate cancer cell growth by inhibiting MAPK pathway. *J Biol Chem* 2005; 280:14325-30; PMID:15805119; <http://dx.doi.org/10.1074/jbc.M413313200>
58. Nakagawa T, Kollmeyer TM, Morlan BW, Anderson SK, Bergstralh EJ, Davis BJ, Asmann YW, Klee GG, Ballman KV, Jenkins RB. A tissue biomarker panel predicting systemic progression after PSA recurrence post-definitive prostate cancer therapy. *PLoS One* 2008; 3:e2318; PMID:18846227; <http://dx.doi.org/10.1371/journal.pone.0002318>
59. Gorlov IP, Sircar K, Zhao H, Maity SN, Navone NM, Gorlova OY, Troncoso P, Pettaway CA, Byun JY, Logothetis CJ. Prioritizing genes associated with prostate cancer development. *BMC Cancer* 2010; 10:599; PMID:21044312; <http://dx.doi.org/10.1186/1471-2407-10-599>
60. Bera TK, Maitra R, Iavarone C, Salvatore G, Kumar V, Vincent JJ, Sathyanarayana BK, Duray P, Lee BK, Pastan I. PATE, a gene expressed in prostate cancer, normal prostate, and testis, identified by a functional genomic approach. *Proc Natl Acad Sci U S A* 2002; 99:3058-63; PMID:11880645; <http://dx.doi.org/10.1073/pnas.052713699>
61. Xu LL, Shanmugam N, Segawa T, Sesterhenn IA, McLeod DG, Moul JW, Srivastava S. A novel androgen-regulated gene, PMEPA1, located on chromosome 20q13 exhibits high level expression in prostate. *Genomics* 2000; 66:257-63; PMID:10873380; <http://dx.doi.org/10.1006/geno.2000.6214>
62. Zhu L, van den Heuvel S, Helin K, Fattaey A, Ewen M, Livingston D, Dyson N, Harlow E. Inhibition of cell proliferation by p107, a relative of the retinoblastoma protein. *Genes Dev* 1993; 7(7A):1111-25; PMID:8319904; <http://dx.doi.org/10.1101/gad.7.7a.1111>
63. Claudio PP, Howard CM, Baldi A, De Luca A, Fu Y, Condorelli G, Sun Y, Colburn N, Calabretta B, Giordano A. p130/pRb2 has growth suppressive properties similar to yet distinctive from those of retinoblastoma family members pRb and p107. *Cancer Res* 1994; 54:5556-60; PMID:7923196
64. Ding Z, Wu CJ, Chu GC, Xiao Y, Ho D, Zhang J, Perry SR, Labrot ES, Wu X, Lis R, et al. SMAD4-dependent barrier constrains prostate cancer growth and metastatic progression. *Nature* 2011; 470:269-73; PMID:21289624; <http://dx.doi.org/10.1038/nature09677>
65. Tai S, Sun Y, Squires JM, Zhang H, Oh WK, Liang CZ, Huang J. PC3 is a cell line characteristic of prostatic small cell carcinoma. *Prostate* 2011; 71:1668-79; PMID:21432867; <http://dx.doi.org/10.1002/pros.21383>
66. Li Y, Wang HY, Wan FC, Liu FJ, Liu J, Zhang N, Jin SH, Li JY. Deep sequencing analysis of small non-coding RNAs reveals the diversity of microRNAs and piRNAs in the human epididymis. *Gene* 2012; 497:330-5; PMID:22313525; <http://dx.doi.org/10.1016/j.gene.2012.01.038>
67. Youssef YM, White NM, Grigull J, Krizova A, Samy C, Mejia-Guerrero S, Evans A, Yousef GM. Accurate molecular classification of kidney cancer subtypes using microRNA signature. *Eur Urol* 2011; 59:721-30; PMID:21272993; <http://dx.doi.org/10.1016/j.eururo.2011.01.004>
68. Ryland GL, Bearfoot JL, Doyle MA, Boyle SE, Choong DY, Rowley SM, Tothill RW, Goringe KL, Campbell IG; Australian Ovarian Cancer Study Group. MicroRNA genes and their target 3'-untranslated regions are infrequently somatically mutated in ovarian cancers. *PLoS One* 2012; 7:e35805; PMID:22536442; <http://dx.doi.org/10.1371/journal.pone.0035805>
69. Devor EJ, Hovey AM, Goodheart MJ, Ramachandran S, Leslie KK. microRNA expression profiling of endometrial endometrioid adenocarcinomas and serous adenocarcinomas reveals profiles containing shared, unique and differentiating groups of microRNAs. *Oncol Rep* 2011; 26:995-1002; PMID:21725615
70. Wang J, Xiang G, Mitchelson K, Zhou Y. Microarray profiling of monocytic differentiation reveals miRNA-mRNA intrinsic correlation. *J Cell Biochem* 2011; 112:2443-53; PMID:21538479; <http://dx.doi.org/10.1002/jcb.23165>
71. Claudio PP, Zamparelli A, Garcia FU, Claudio L, Ammirati G, Farina A, Bovicelli A, Russo G, Giordano GG, McGinnis DE, et al. Expression of cell-cycle-regulated proteins pRb2/p130, p107, p27(kip1), p53, mdm-2, and Ki-67 (MIB-1) in prostatic gland adenocarcinoma. *Clin Cancer Res* 2002; 8:1808-15; PMID:12060621
72. Yang G, Yang X. Smad4-mediated TGF-beta signaling in tumorigenesis. *Int J Biol Sci* 2010; 6:1-8; PMID:20087440; <http://dx.doi.org/10.7150/ijbs.6.1>
73. Arroyo JD, Chevillet JR, Kroh EM, Ruf IK, Pritchard CC, Gibson DF, Mitchell PS, Bennett CF, Pogosova-Agadjanian EL, Stirewalt DL, et al. Argonaute2 complexes carry a population of circulating microRNAs independent of vesicles in human plasma. *Proc Natl Acad Sci U S A* 2011; 108:5003-8; PMID:21383194; <http://dx.doi.org/10.1073/pnas.1019055108>